AD-A096 627 TEXAS UNIV AT AUSTIN F/G 11/4
THE INTERFACE STRUCTURE IN GRAPHITE/ALUMINUM COMPOSITES,(U)
1980 S TSAI, M SCHMERLING, H L MARCUS N00014-78-C-0094

UNCLASSIFIED NL

1 OF 1
AD A
096627

END
DATE
FILMED
4-81
DTIC

LEVEL II

TO BE PUBLISHED IN CERAMIC ENGINEERING AND SCIENCE PROCEEDINGS

(11) 1980

(6) THE INTERFACE STRUCTURE IN GRAPHITE/ ALUMINUM COMPOSITES

Contract ~~N00014-78-C-0094~~

(12) 22

Swe-Den Tsai, Michael Schmerling Harris ~~and H.~~ L. Marcus
Mechanical Engineering/
Materials Science and Engineering
The University of Texas
Austin, TX 78712

Abstract

Transmission electron diffraction and Auger electron spectroscopy studies of the interfaces of selected graphite/ aluminum composite systems revealed that generally titanium diboride, (TiB_2), and aluminum oxide, (Gamma-Al_2O_3), were present as the interfacial phases. The grain size and the crystallographic structure of these interfacial phases were studied and are discussed in terms of the transverse fracture behavior of the graphite/aluminum composites.

Introduction

The graphite fiber reinforcement/metal matrix composites are of great interest because of their high strength and potential for large-scale production and use. Aluminum alloys appear promising as matrix materials for graphite reinforced metal. In the majority of cases the fiber is pretreated followed by controlled immersion into molten aluminum to make the metal matrix composite [1]. Even as this liquid metal infiltration technology advanced, the transverse strength of graphite-aluminum composites remained poor in contrast to the high strength in the longitudinal direction. A recent study [2] indicated that the transverse behavior should be closely related to the interfacial properties. This interface could be the reaction zone between aluminum and fiber or the reaction zone between pretreatment coating and either the fiber or matrix.

Some variations in the treatment of graphite fibers have been developed [3], and the transverse strength has been improved without significant degradation of the longitudinal strength. But the basic understanding of the crystal structure of the interface phases is still lacking.

The aim of the present work was to obtain crystallographic information about the interface reaction zone using electron diffraction in a Transmission Electron Microscope

(TEM). The corresponding interface chemistry on some specimens was studied using a Scanning Auger Microscope (SAM). Various composite materials with different transverse strengths were employed in order to correlate the structure of interface phase with mechanical properties.

Titanium diboride (TiB_2) was found in the interface layer for every material processed by the standard pretreatment coating. γ-Aluminum oxide (γ-Al_2O_3) phase was also observed in most materials studied here as were other oxides and carbides.

Experimental

The graphite/aluminum composite materials examined in this study are listed in Table 1 along with fiber type, transverse strength and the interface phases observed in TEM. Except for G3842 which is plate consolidated from T133 wire, the materials are all unconsolidated wires. The matrix material is 6061 Al. The single fiber wire in Table 1 is a single graphite fiber "prepreg" with no pretreatment coating on the interface. This composite wire is produced by the ion vapor deposition of an aluminum 4% Mg alloy on the fiber. Basically, two fiber types were examined in this study, each representing currently available commercial forms. One is a low modulus type II PAN fiber with the oriented graphite basal planes tending to be parallel to the fiber

surface just below it. The other is a high modulus pitch type fiber with basal planes roughly perpendicular to the fiber surface. All fibers have circular cross sections. See Figure 1 for the relative basal plane orientation.

To make the fiber-matrix interface accessible to observation, a selective etching method was used. The materials were dipped or swabbed in one of three different etchants: a concentrated HCl solution, an HCl solution diluted by 60-70% volume percent methanol, and a 7N KOH solution. The samples were then thoroughly rinsed with acetone, methanol or ultrasonically cleaned in methanol. Thus, the sample fibers were free of the aluminum matrix material and only some interface pieces still attached to the fiber surface were left. Searching along the fiber surfaces in the transmission electron microscope* revealed numerous interface pieces thin enough for transmission in the samples prepared in HCl solution diluted by methanol or in concentrated HCl solution and a few thin interface layers in the sample etched by KOH.

Both the composite wire and plate were fractured in situ in the Scanning Auger Microscope (SAM)** under 10^{-3} μPa vacuum

*A JEOL 150 KeV TEM was used in the transmission diffraction studies.

**The SAM instrument applied in these studies was the Physical Electronics model 590 system.

in order to unambiguously analyze the material in the fractured interface region between fiber and matrix. In addition, some of the samples were sputtered using 5kV argon ions and examined to identify the chemical species present. An electron beam spot size of appoximately 1μ or less was used to give good spatial resolution and high signal to noise ratio.

Results and Discussion

The most often observed phase was a TiB_2 hexagonal structure which was found in all the pretreated materials studied here. Some typical electron diffraction patterns of TiB_2 prepared in HCl plus methanol for various composite materials are shown in Figure 2. The observation of the spotty nature of the rings in the TiB_2 diffraction pattern from the T114A composite indicated that the grain size of TiB_2 in the T114A composite was larger than the grain size of TiB_2 in the other composites studied here. This grain size difference was consistently observed in many fibers and also in samples prepared by the other selective etchants: concentrated HCl and KOH. One basic difference between T114A and the rest of the composite materials is that the fiber in T114A has the graphite basal plane parallel to the fiber surface but the other composites have the pitch type fiber with basal plane perpendicular to the surface. This difference in

crystallographic orientation in the substrate may lead to a preferential growth of large grains for a TiB_2 reaction product in T114A. The grain size effect may play a role in the transverse properties of the composites.

In recent years it has been demonstrated that a high degree of preferred orientation of "fibrils" are formed in the graphite fiber of high tensile modulus and strength[4]. The "fibril" is a structural unit which is composed of "microfibrils" and pore structure[5,6]. Its dimensions have been estimated to be from 250Å to as high as 1000Å[7,8] in the transverse direction. The fibrils have indefinite length and may form a continuous or branched network. The "microfibril" is a stacking of graphite layers and the dimensions can be characterized by the stacking height (or the microfibril thickness) and the microfibril width and length.

A close investigation into the morphology of TiB_2 layer in electron micrographs for various composites showed some striated or ripple characteristics of this interface layer in pitch fiber reinforced materials (see Figure 3). These ripples are probably due to the "fibril" structure. The chemical vapor deposited TiB_2 covers the fiber surface as a surface replica. A rough estimation of the dimension across these strips gives values ranging from 200Å to 600Å which are in the range of fibril transverse dimension.

The micrographs of TiB_2 layer formed at the interface for low modulus PAN II composites are also shown in Figure 4. The comparison between pitch fiber and low modulus PAN II composites can be seen in Figure 3 and Figure 4, respectively, where the TiB_2 phase with crenulations or ripples for VSB 32 pitch type composites and without for PAN II type composites are presented. The diffraction pattern of Figure 3 (c,d) is shown in Figure 2 (b) and that of Figure 4 is shown in Figure 2(c).

An aluminum oxide (γ-Al_2O_3) phase was often observed along the fiber/matrix interface. The origin of the oxide has not been clearly established, but it is most likely the reaction product of oxygen which was contained in the fibers and then segregated to the interface during the aluminum-infiltration processing step. The exact role of this oxide layer is not known at present, but the recent SAM studies[9] indicate that it seems to promote matrix adhesion to the graphite which might be responsible for an increased transverse strength in graphite/aluminum composites. The present TEM examination of these oxide layers on the fiber surfaces indicated that the γ-Al_2O_3 phase has a relatively larger grain size on the average than that of TiB_2. The electron diffraction patterns of γ-Al_2O_3 (Fig. 5) were observed for the composites with an interface coating and the single fiber wire which had no coating on the interface.

It is also interesting to point out that titanium carbide, TiC, was observed in G3842 and G3636 composites. In both materials, the rings of diffraction pattern are continuous, however the diffraction ring is broadened to some extent in G3636 composite. This is believed to be due to the effect of very fine grain size. The diffraction pattern and micrograph for the TiC phase can be seen in Figure 7.

The Al_4C_3 phase which was determined[10] to be present at the interface in other research (Aerospace Corp.) could not be identified by the technique used here, because Al_4C_3 is decomposed in water and highly soluble in both acid and alkali solution. Recently Al_4C_3 as well as oxides other than Al_2O_3 have been observed using an electrochemical thinning technique. Further studies using this approach are now in progress.

The interface reaction zone in the composites studied in the TEM was also investigated by SAM combined with in situ fracture to help identify the interface chemistry. The fracture paths were through the oxide layer or close to either the fiber side or matrix side of the interfaces. The Auger chemical analysis versus the depth into the fracture surface was obtained using inert argon ion sputtering. Using sensitivity factors[11] estimation of the atomic concentration ratio of titanium to boron, Ti/B at selected points after

sputtering was consistently about 0.51-0.57 in the G3636 and G3842 materials (see Figures 8 and 9). A standard TiB_2 Auger spectra after sputtering of TiB_2 powder is shown in Fig. 10. The Ti/B ratio is ~.55. A lack of chemical shift in peak location and consistent peak to peak height analysis together with the assumptions that the escape depth correction, back scattering factor and surrounding chemical effect are negligible, support the TEM results that TiB_2 phase was present in the interface layer. Further studies are being conducted in the TEM and SAM to clarify and extend the results reported in this paper.

Conclusions

Results of this work can be summarized as follows:

1. TiB_2 phase is generally present for the aluminum/graphite composites processed by standard pretreatment coating technology.
2. Larger TiB_2 phase grain size was observed in PAN II fibers with the graphite basal plane perpendicular to the fiber surface. This could relate to higher transverse strength in composites with this fiber.
3. γ-Al_2O_3 phase was found in most composites and is relatively larger in grain size than the TiB_2 phase.

4. The mixture of γ-Al_2O_3 and TiB_2 was observed in some areas of interface for the composite with pitch fibers.
5. AES identified the existence of the approximately stoichiometric TiB_2 atomic concentration ratio, for many of the composites studied.

Acknowledgement

This research was sponsored by the Office of Naval Research, Contract N00014-78-C-0094 at The University of Texas at Austin.

References

1. Dull, D.L. and Amateau, M.F., "Transverse Strength Properties of Graphite-Aluminum Composites," Quarterly Progress Report No. 1, TOR-0077 (2726-03)-1, The Aerospace Corporation, El Segundo, CA (10 Jan, 1977).

2. Steckel, G.L., Flowers, R.H. and Amateau, M.F., "Transverse Strength Properties of Graphite-Aluminum Composites," Final Report for Period 1 Oct. 1977 - 30 Sept. 1978 for Naval Surface Weapons Center, TOR-0078 (3726-03)-4, Sept. 30, 1978.

3. Amateau, M.F., "Progress in the Development of Graphite-Aluminum Composites Using Liquid Infiltration Technology," Journal of Composite Materials, Vol. 10, Oct. 1976, p. 279.

4. Fourdeux, A., Herninckx, C., Perret, R. and Ruland, W., Comt. Rend. 269C, (1969), 1597.

5. Badami, D.V., Joiner, J.C. and Jones, G.A., Nature 215, (1967) 386.

6. Johnson, W. and Walt, Nature 215 (1967) 384.

7. Johnson, J.W., Rose, P.G. and Scott, G. in 3rd Conf. on Industrial Carbon and Graphite (1970), London, (pub. 1971), p. 443.

8. Bacon, R. and Silvagge, A.F., Carbon 9 (1971), 321.

9. Marcus, H.L., Dull, D.L. and Amateau, M.F., "Scanning Auger Analysis of Fracture Surfaces in Graphite-Aluminum Composites," in Failure Modes in Composites IV, J.A. Cornie and F.W. Crossman, eds. Conference Proceedings, The Metallurgical Society of AIME, Fall 1977.

10. Padlla, F., Harrigan, W.C., Jr., and Amateau, M.F., "Handbook of Test Methods for Evaluation and Qualification of Aluminum-Graphite Composite Materials," Material Sciences Laboratory, The Aerospace Corp., El Segundo, CA (21 Feb. 1975).

11. Davis, L.E., et al, Handbook of Auger Electron Spectroscopy, Published by Physical Electronics Industries, 2nd edition, 1976.

Table 1

Composite Materials	Graphite Fiber Type	*Transverse Strength MPa	**Phase(s) Observed in TEM
T114A	PAN II (Celion 6000)	76	TiB_2, γ-Al_2O_3
G3842 (made from T133)	Pitch (VSB-32)	31	TiB_2, γ-Al_2O_3, TiC
G3636 (made from T105A)	Pitch (VSB-32)	10	TiB_2, γ-Al_2O_3, TiC
T109B	Pitch (VSB-32)	not available	TiB_2
HM pitch/ 6061	HM 3000	14-80 depends on consolidation process	TiB_2
Single Fiber Wire	PAN II (Celion 12000)	not measured	γ-Al_2O_3

*Transverse Strength was tested in plate forms by Aerospace Corporation.

**Camera constant used here for d-space identification was about 1.37 Ångstrom-cm.

PAN

PITCH

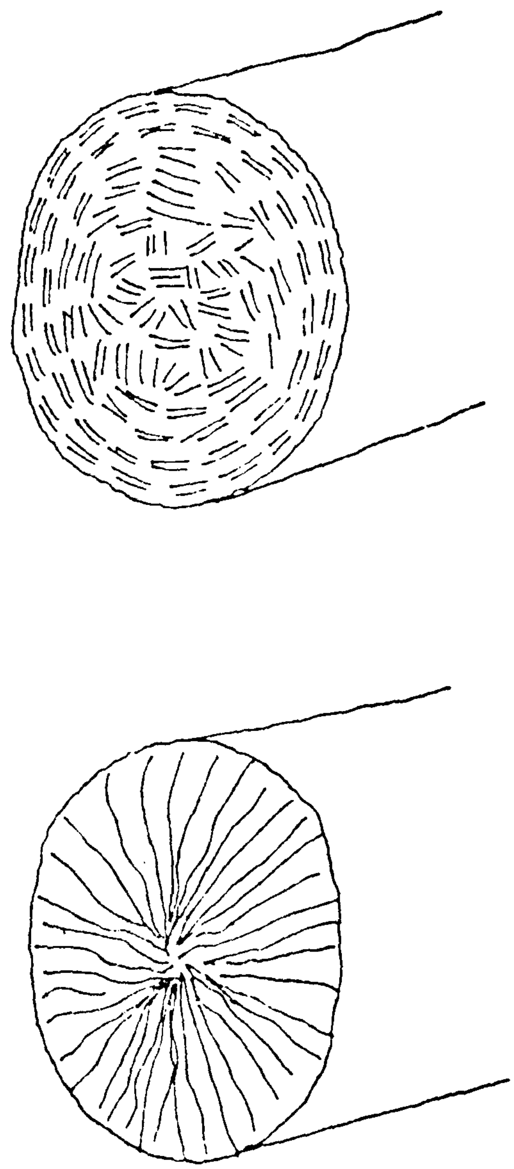

Fig. 1. Schematic diagram of oriented structure in PAN and Pitch type fibers.

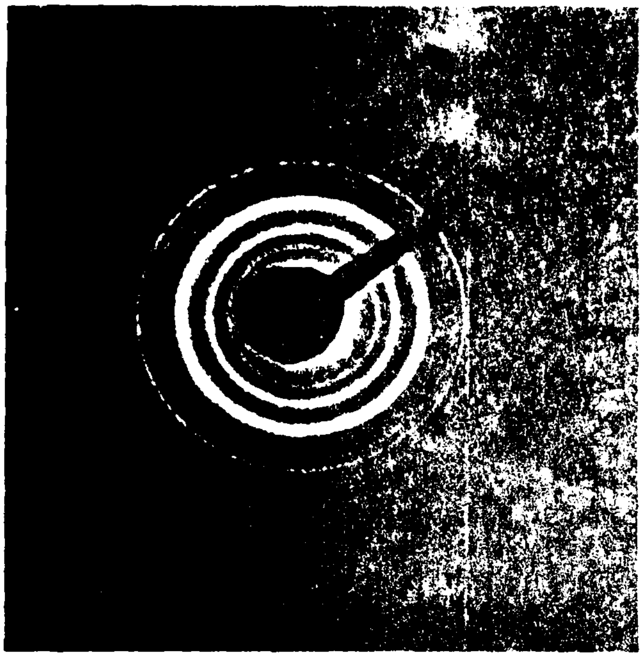

(a)

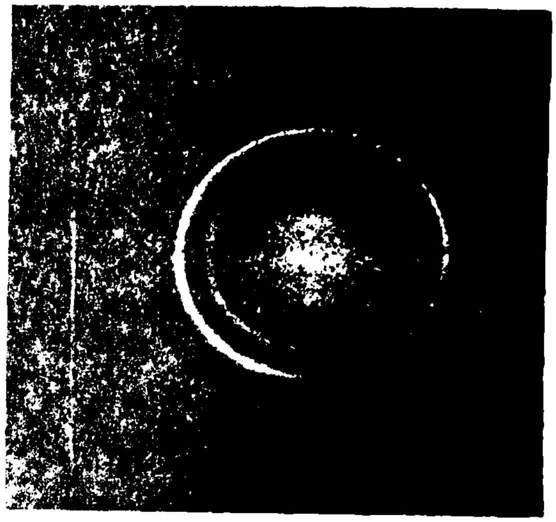

(b)

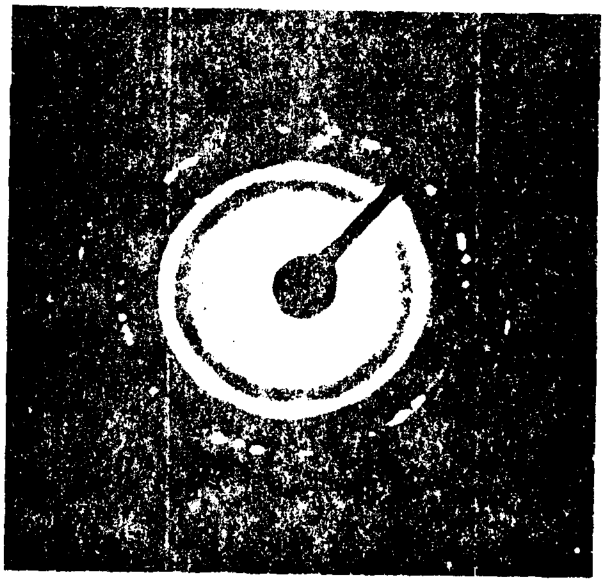

(c)

Fig. 2. Electron diffr[illegible] pattern [illegible]
(a) G[illegible] [illegible] [illegible]
HCl and [illegible]

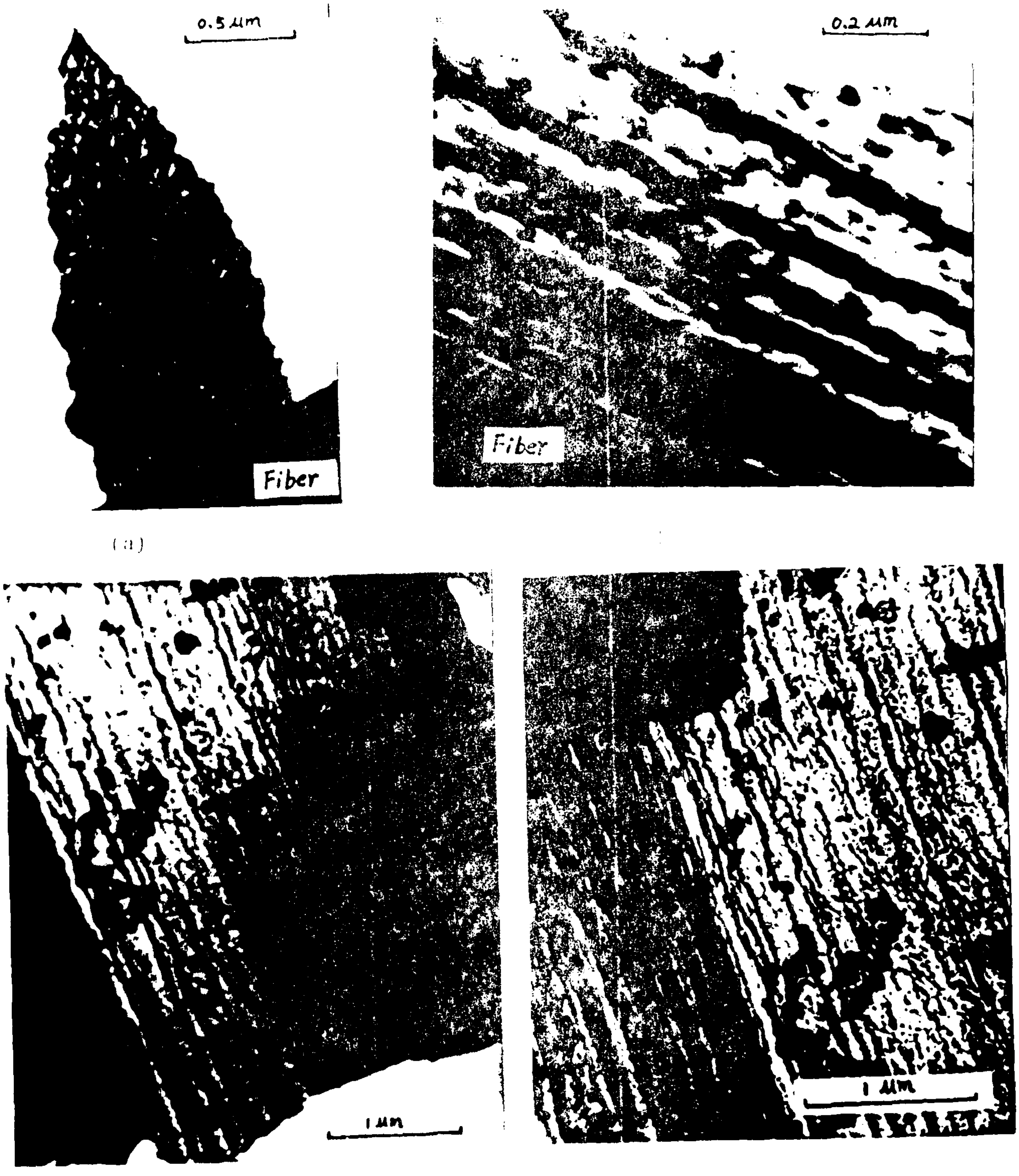

(a)

(c)

(d)

Fig. 3 Electron micrographs [illegible] layers in various [illegible] (a) [illegible] (d) G3842 [illegible]

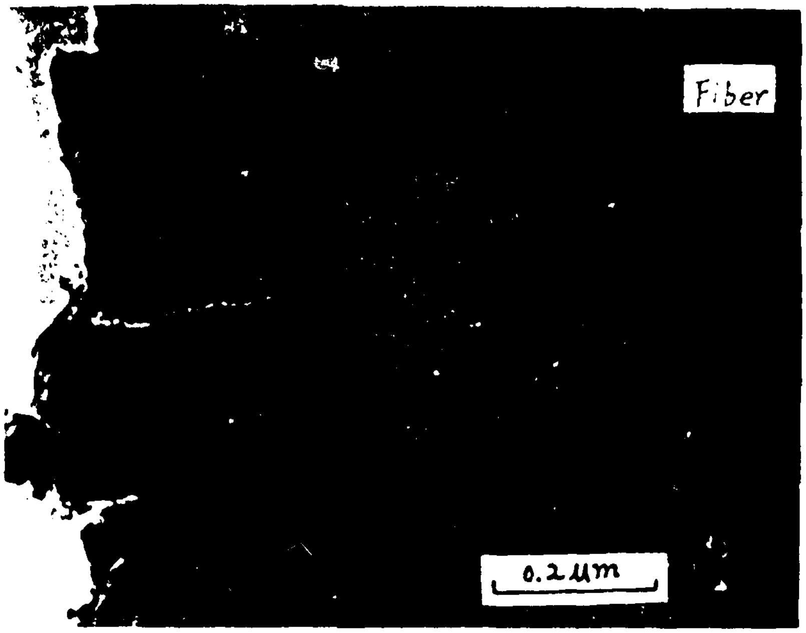

(a)

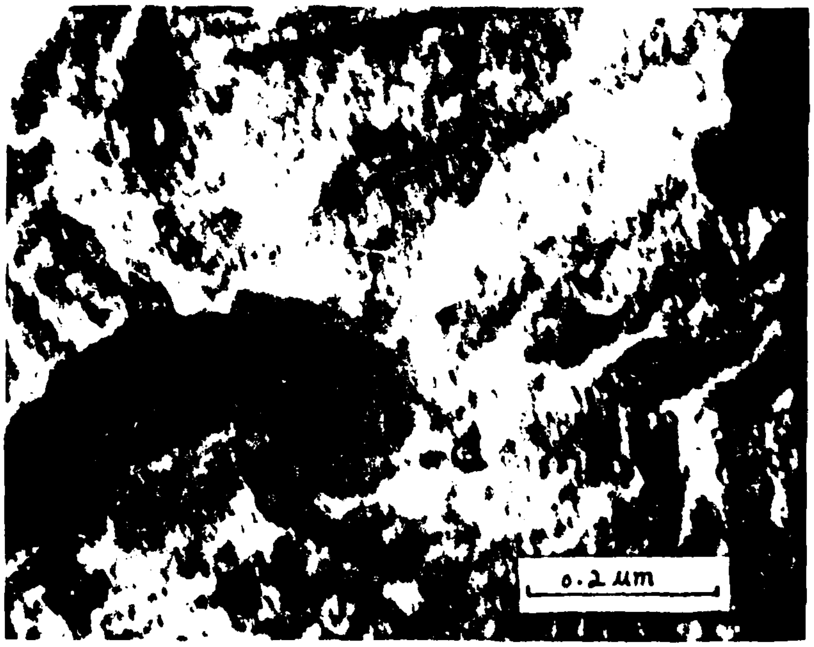

(b)

Fig. 4. Electron micrographs of larger grain size TiB_2 phase in TI14A (a) sample etched by KOH, (b) sample etched by HCl and methanol.

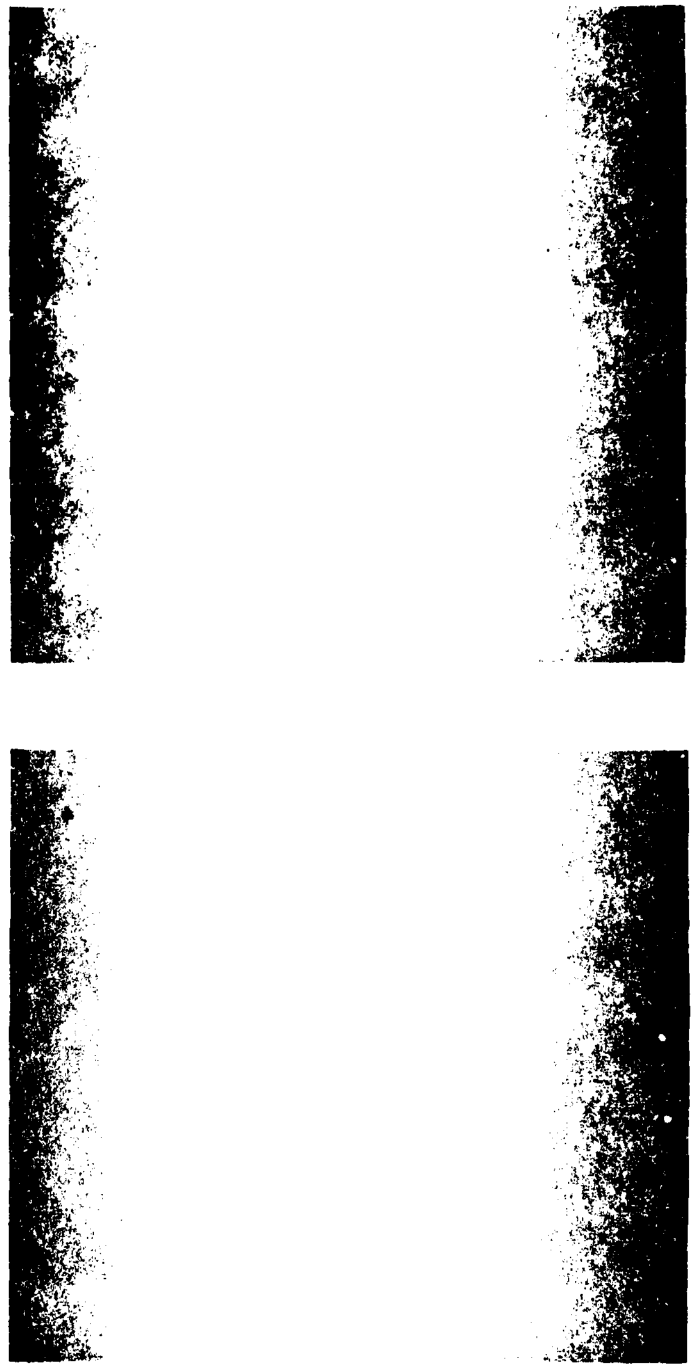

Fig. 5. Electr... phase.
(a) ... d by HCl
and met... is also
present

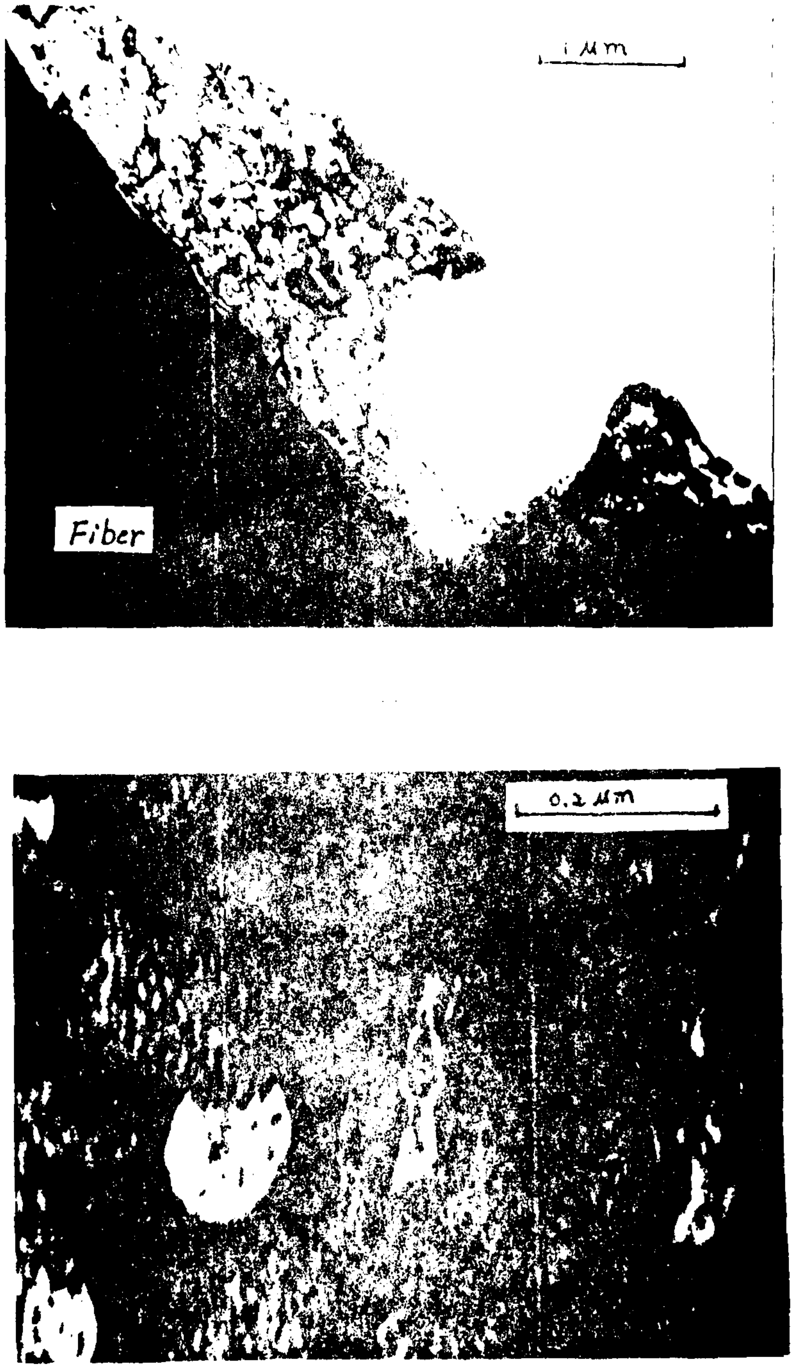

Fig. 6. Micrographs [illegible] 114A etched by HCl and [illegible] of whole piece, the dark part [illegible] magnification of center area of [illegible] Note: Some larger grain [illegible] neck part of the whole pi[illegible]

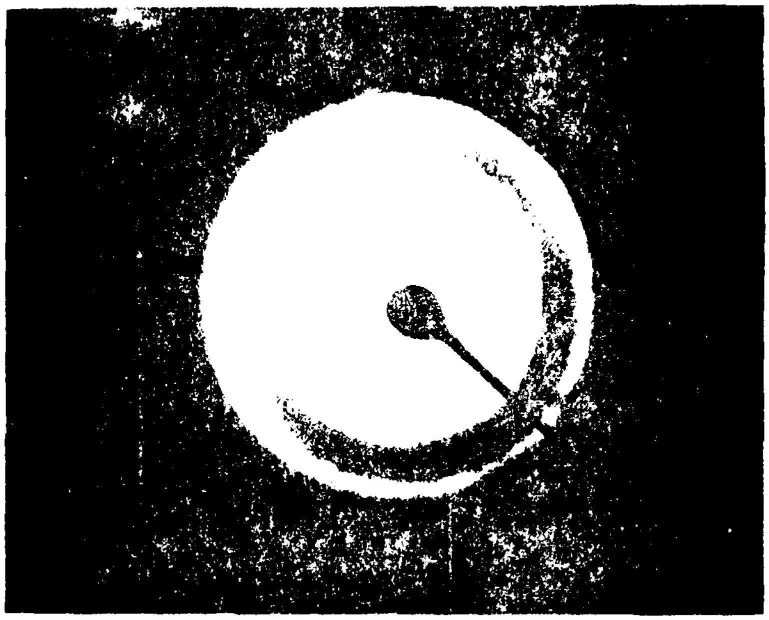

Fig. 7. The [illegible] (a) a diffused electron [illegible] micrograph of (a).

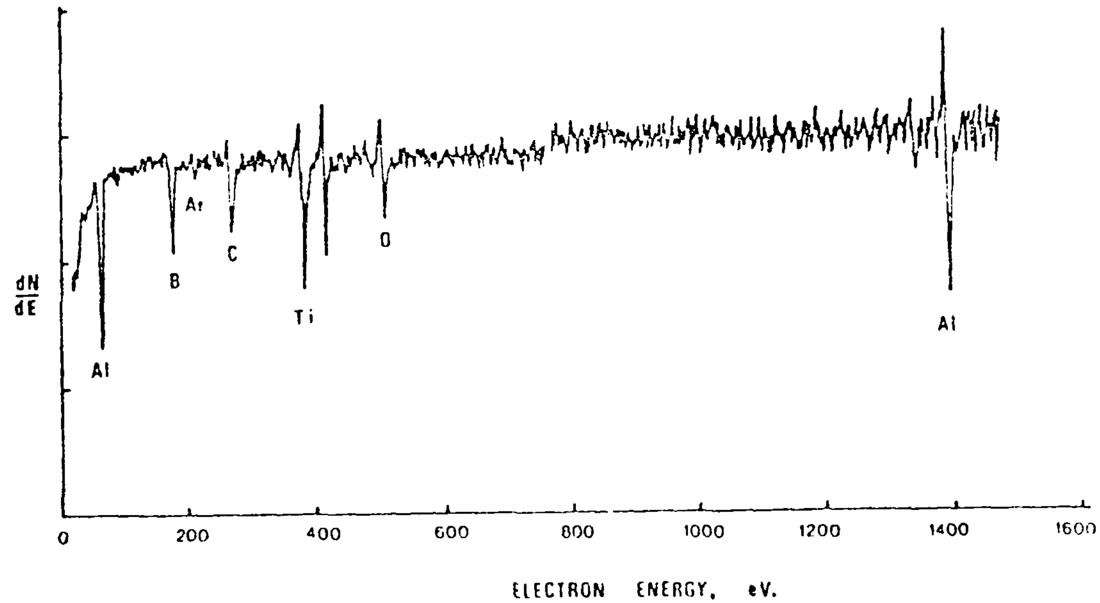

Fig. 8. AES analysis of the fractured interface after 25 minute sputtering in T105A (plate G3636 was used).

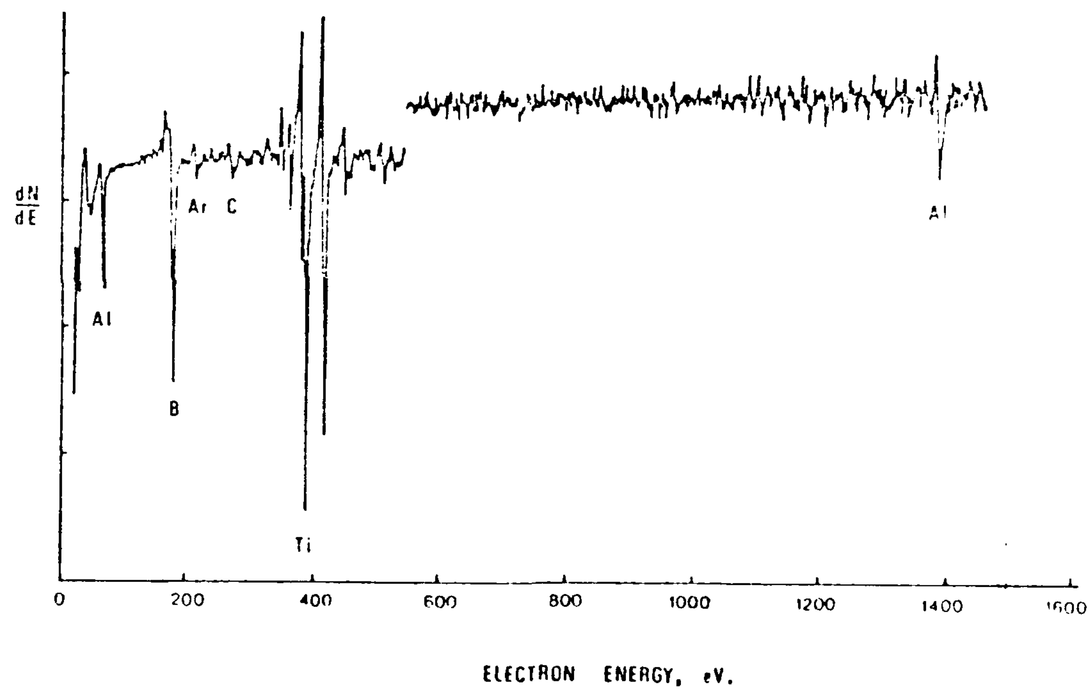

Fig. 9. AES analysis of the fractured interface after 5 minute sputtering in G3842.

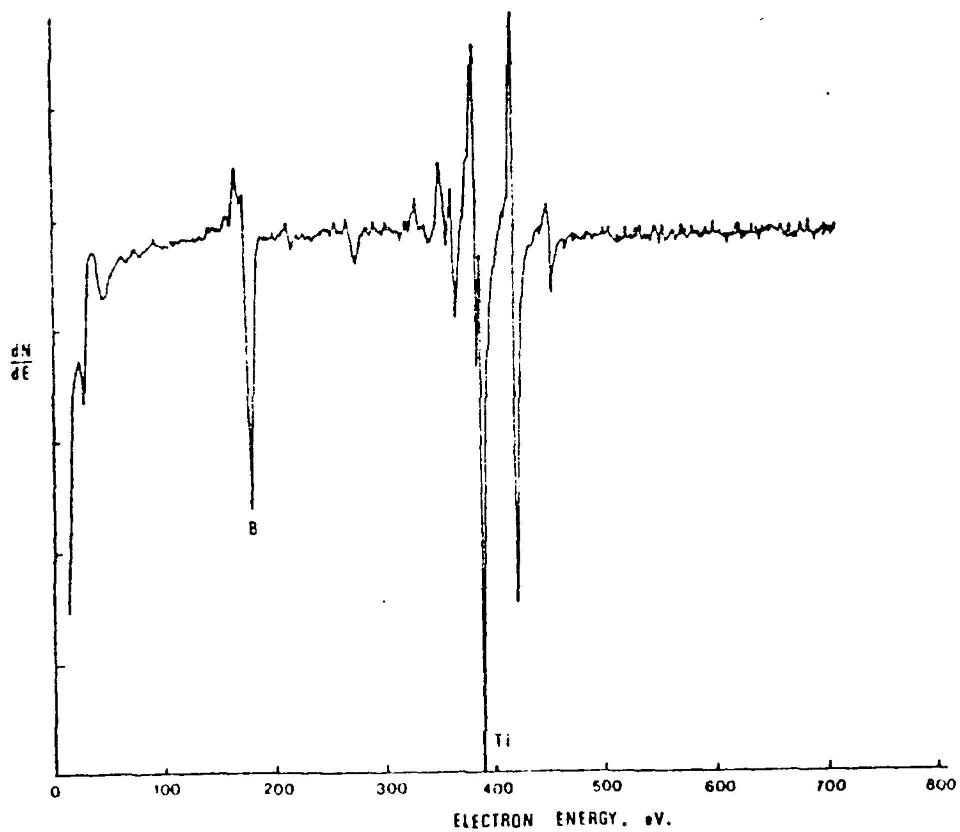

Fig. 10. Standard TiB_2 SAM spectra after sputtering.